

Influence of roughness in ultrasonic welding of carbon fiber/PEEK composites

CARASSUS Fabrice^{1,2,a*}, KORYCKI Adrian^{1,2,b}, GARNIER Christian^{1,c},
CHABERT France^{1,d}, YAHIAOUI Malik^{1,e} and DJILALI Toufik^{2,f}

¹LGP-ENIT-INPT, University of Toulouse, 47 Avenue d'Azereix, 65016 Tarbes, France

²LAUAK FRANCE, 8 Rue Louis Caddau, 65000 Tarbes, France

^afabrice.carassus@groupe-lauak.com, ^bakorycki@enit.fr, ^ccgarnier@enit.fr, ^dfchabert@enit.fr,
^emyahiaoui@enit.fr, ^ftoufik.djilali@groupe-lauak.com

Keywords: Ultrasonic Welding, Composites, Roughness, Shear Strength

Abstract. In this work on ultrasonic welding of CF/PEEK composites, it was established that the surface roughness of the substrates has an influence on the interfacial strength of a joint. The joint resistance is lower when the roughness increases. Interestingly, a new characteristic time was found, named the healing plateau time (t_{HP}), which is determined by the displacement versus time curves during ultrasonic welding. This time seems to be related to the shear strength of the joint. This is a major finding, because it appears as a non-destructive way of predicting the quality of welds. Besides, DNS test on CF/PEEK unidirectional composite pointed out 40% higher shear strength compared with SLS, performed on CF/PEEK substrates assembled with a 250 μm PEI integrated energy director. Ultrasonic welding was optimized to reach a performance close to the shear strength of bulk.

List of abbreviations

CF	Carbon fiber	QDNSS _{max}	Quasi double-notched shear strength maximum value
D _h	Healing degree	Ra	Profile's arithmetic mean deviation
D _{IC}	Intimate contact degree	Rz	Average profile height
DNS	Double-notch shear	SDB	Sandblasted
G _{IC}	Mode I energy release rate	SLS	Single lap shear
G _{IC(∞)}	Bulk material resistance	SS	Shear strength
G _{IIC}	Mode II energy release rate	SS _{bulk}	Bulk material shear strength
HP	Healing plateau	STB	Shotblasted
LSS	Lap shear strength	STD	Standard
LSS _{max}	Lap shear strength maximum value	t _h	Healing time
$\lambda_{\text{cut-off}}$	boundary wavelength between roughness and waviness	t _{HP}	Healing plateau time
PEEK	Polyetheretherketone	t _{ic}	Intimate contact time
PEI	Polyetherimid	t _{rep}	Reptation time
QDNSS	Quasi double-notched shear Strength	USW	Ultrasonic welding

Introduction

Composites in aeronautics are currently dominated by thermosets, but the development of high-performance thermoplastic composites is booming. These materials open the way towards new forming and assembling processes. *Ultrasonic welding* (USW) is a joining method that uses ultrasonic vibrations and pressure over time to generate heat at the contact surfaces. Joining is achieved by the formation of a molten interphase which consolidates on cooling under pressure. The use of an energy director, a pure polymer film between both surfaces to be welded, facilitates the surface wetting to achieve intimate contact. *Polyetherimide* (PEI) is often used as energy director for joining *Polyetheretherketone* (PEEK) matrix composites, as both polymers are miscible. Moreover, PEI has the advantage of flowing at a lower temperature than PEEK, which facilitates the mobility of its macromolecular chains through PEEK.

The weld quality in USW depends on several process parameters and material properties, but geometric parameters must also be considered. Besides, interface healing and intimate contact between both surfaces to be welded are still not fully understood. According to Voyutskii [1], surface wetting is not sufficient to develop interfacial strength in polymer welding, the chains must be able to diffuse from one surface to another. Before the polymer chains diffuse from one side to the other one, intimate contact is established by the flow of asperities onto the surface of polymeric materials. Then, healing is generated by the chains diffusing across the interface and their random rearrangement. The highest welding strength is achieved when healing is completed and the interface disappears completely. Intimate contact describes the evolution of physical contact between both materials to be welded. It represents the true contact surface, formed by the asperities in contact, in opposition to the apparent contact surface. Initially, a perfect contact is impossible because of the surface roughness. It is assumed that roughness improves the frictional effect in USW and increases the temperature at the interface. But on the other hand, the imperfections must be flattened under pressure to generate intimate contact. Indeed, the intimate contact is the necessary condition for the polymeric chains to diffuse across the interface. The effect of roughness on weld strength is rarely considered and to date, no experimental study of roughness in USW is available. Usually, the specimens to be welded are prepared from plane plates without considering their roughness. However, various surface qualities are obtained when parts are manufactured in industrial conditions. Therefore, a deeper knowledge is needed to weld despite imperfect geometry or unusual roughness. Some analytical approaches were developed to handle this topic. In the most advanced existing models, the *intimate contact degree* (D_{IC}) has been established by considering the roughness as a set of rectangular asperities [2,3], far from realistic geometry. However, this model may be sufficient to predict the influence of roughness on the joint quality, by linking the roughness parameters to pressure, viscosity and welding time. Further refinement of models may be interesting to fit the realistic roughness parameters. Anyway, such models must be validated with experimental data, which are the purpose of this article.

This work aims to contribute to the prediction of the weld resistance in USW according to the initial part roughness. Thus, the influence of roughness on the interfacial strength is investigated by combining mechanical characterization and analytical approach. Most studies choose the *mode I energy release rate* (G_{IC}) to evaluate the adhesion of an assembly composed of 2 bulk materials [4,5,6]. This energy release rate could be considered as the resistance of welds. It can be compared to the $G_{IC(\infty)}$ corresponding to the bulk material resistance. This energy release rate, attributed to a multiplicative combination of interfacial and bulk effects depends on the adhesion time [7]. Eq. 1 relates it directly to the polymer *reptation time* (t_{rep}). t_{rep} mainly depends on the temperature and the polymer chain hindrance (Eq.2). It defines the average time needed for a polymer chain to completely leave its initial position. The latter is represented in the reptation theory by a tube from which the macromolecule escapes at the extremities.

$$\frac{G_{IC}(t)}{G_{IC\infty}} \approx \left(\frac{t}{t_{rep}}\right)^{\frac{1}{4}} \tag{1}$$

$$t_{rep} = \frac{N^3 l_0^3 \mu_M}{N_e k_B T} \tag{2}$$

With: N number of monomers, l_0 segment length of an ideal chain, μ_M dynamic viscosity, N_e number of monomers between entanglements, k_B Boltzmann constant

In the aerospace industry, it is customary to consider the shear strength of joints instead of energy release rate. It was therefore decided to implement a new approach based on the mode II resistance and to discuss its validity while quantifying the influence of roughness.

Materials and Methods

USW was performed in displacement mode using a Mecasonic Omega 4x pneumatic welding machine. The input parameters were the applied pressure, the amplitude and the sonotrode displacement. Time, displacement, and energy dissipation were recorded by the device during welding. Fig. 1 shows the general layout of the welding system.

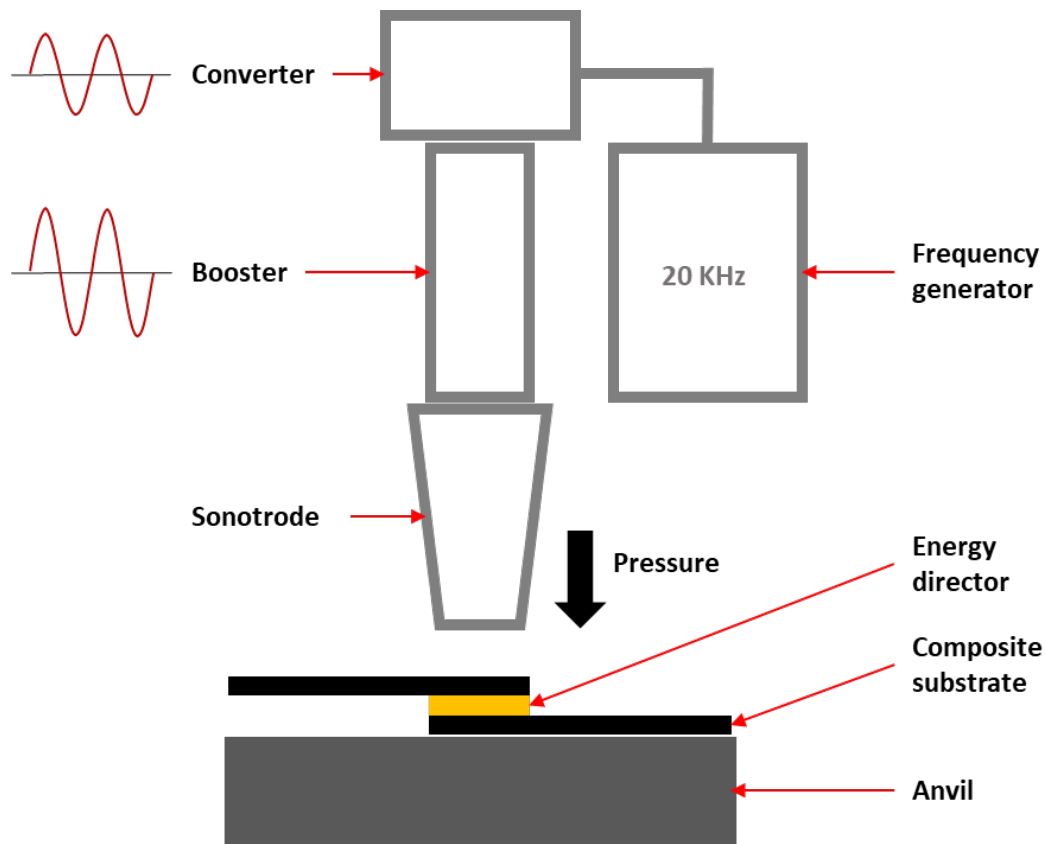


Fig. 1. Layout of the ultrasonic welding device.

Composite plates were manufactured with a Pinette Emidecau Industries Lab800 thermo-compression device. The substrates were made of APC-2 prepreg supplied by Solvay, which is composed of unidirectional *carbon fibers with polyetheretherketone matrix (CF/PEEK)*. Composite plates underwent an additional step to integrate a 0.25 mm thick pure polymer film of Ultem 1000 PEI as energy director under compression. To vary the surface finish of these composite plates, steel backplates of different roughness were used. Several surface conditions were tested to obtain different types and values of roughness.

The composite plates were then cut in 100 x 25 x 2 mm substrates. Before welding, their roughness was measured using a Mahr MarSurf PS1 roughness meter, by averaging 5 measurements spread over the area to be welded, in the longitudinal direction on each sample. A comparison between the *profile's arithmetic mean deviation* (Ra) (Eq. 3) and the *average profile height* (Rz) was carried out but did not show a significant difference. Therefore, Ra was chosen as the default measurement parameter. In accordance with roughness tables, the *boundary wavelength between roughness and waviness* ($\lambda_{\text{cut-off}}$) was chosen to be 0.8 mm for roughness below 2 μm , and 2.5 mm for roughness above 2 μm . The limited size of the specimens welded area made it inadequate to take higher values of $\lambda_{\text{cut-off}}$.

$$Ra = \frac{1}{n} \sum_{i=1}^n |Y_i| \tag{3}$$

With: Y_i deviations of the evaluation profile from the surface mean line.

Two types of mechanical tests are carried out for this study: The specimens were prepared according to, *Double-Notch Shear* (DNS) testing from ASTM D-3846 and *Single Lap Shear* (SLS) testing from ASTM D-1002.

DNS testing specimens measuring 79.50 x 12.70 x 4.05 mm were cut from a plate with all unidirectional fibers oriented in the direction of the compressive load. The specimens were then double-notched. The tests were conducted on a special compression device as shown in Fig. 2A, which allows the specimen to be held vertically without buckling. A micro-torque spanner was required to tighten the equipment's nuts up to 0.1 N.m. In addition, welded specimens were cut to DNS dimensions to characterize assemblies. To compensate the offset, a counterpart of the same material, with same thickness, was glued to each side of the assembled specimen.

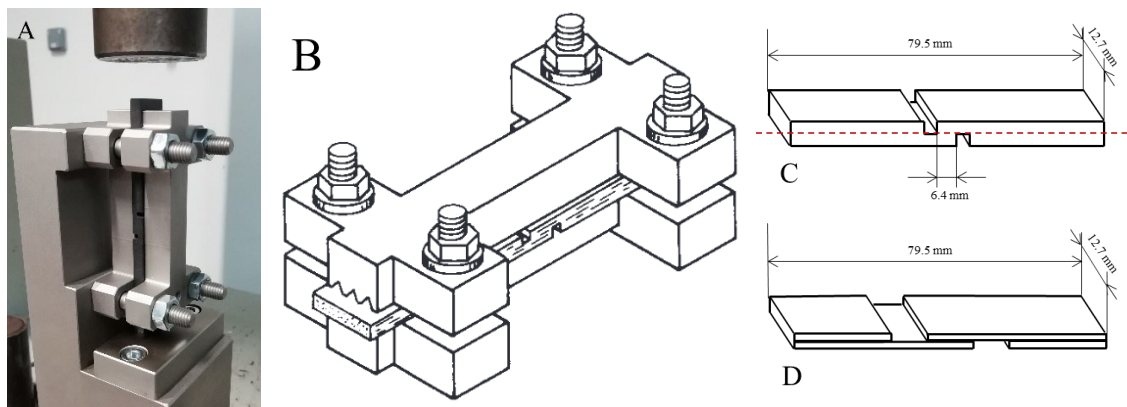


Fig. 2. (A) DNS testing equipment on CF/PEEK composite, (B) scheme of the DNS equipment according to ASTM D-3846, (C) Standard DNS specimen, (D) Quasi-DNS welded specimen.

Then, SLS testing were performed on welded specimens as shown in Fig. 3. An Instron 33R4204 tensile machine with a 100kN cell and adjustable jaws were used. Specimen shear resistances were evaluated, and the fractured surfaces were examined.

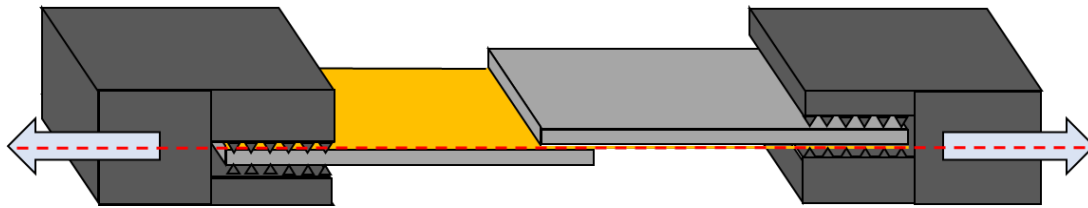


Fig. 3. Principle of the SLS test performed on a CF/PEEK composite with PEI energy director integrated on each welding surface.

Results and Discussion

Rather than establishing a *mode II energy release rate* (G_{IIC}) based on Eq. 1, we chose to compare the *shear strength* (SS) of a joint to the *shear strength of the bulk material* (SS_{bulk}) which is considered to be the maximum shear strength reachable. This ratio could be considered as the *healing degree* (D_h) of the joint and it can be related to the reptation time of the polymer (Eq. 4).

$$\frac{G_{IIC}(t)}{G_{IIC\infty}} \approx \frac{SS(t)}{SS_{bulk}} \approx \left(\frac{t}{t_{rep}}\right)^{\frac{1}{4}} = D_h \quad (4)$$

DNS tests gave a SS_{bulk} value of 73 ± 5 MPa, which is the shear strength value of the bulk material. It is assumed that the strength of assemblies could not reach those of the bulk, due to different entanglement rate in the interface vicinity. It does not mean the quality of assemblies is poor. The welds obtained with optimized welding parameters were characterized. The strength of the bulk was compared with our best assembly configuration by SLS and by a quasi-DNS method, where the assemblies were adapted to fit into the DNS tooling provided. For this comparison, only joints that led to composite fracture were considered. The DNS and SLS tests were performed on a set of 5 specimens, a smaller number for the quasi-DNS test, as several samples were rejected due to failure in the energy director. The advantage of the quasi-DNS test is that the assembly is placed in a pure shear configuration. For the rest of the study, shear strength obtained by SLS test are called Lap Shear Strength (LSS) while strength obtained by quasi-DNS are called Quasi Double Notched Shear Strength (QDNSS). The mean and maximum values for these tests are given in Table 1. The results obtained for both tests are different, +40 % for $QDNSS_{max}$ compared to LSS_{max} , confirming that SLS test does not only imply Mode II fracture. This difference suggests that DNS testing is a more reliable method for the determination of mode II strength than SLS.

The healing degree determined by the $QDNSS/SSB$ ratio is $D_h = 93.7$ %, which means that the welding parameters were fully optimized. This healing degree should be studied further to see whether it is suitable to define the quality of a joint. Similarly, it would be possible to set a performance ratio for the SLS test. LSS/SS_{bulk} ratio is close to 60 %. Consequently, reaching this value in SLS tests could mean a very good performance is achieved for such assembly. Thereafter, it should be difficult to go beyond this LSS_{max} in SLS testing with the same materials.

Table 1. Shear strength values of CF/PEEK composite assemblies with PEI energy director. LSS is obtained by SLS testing and QDNSS is obtained by quasi-DNS testing method. LSS_{max} and $QDNSS_{max}$ are the maximum values of the corresponding tests.

SSB [MPa]	LSS [MPa]	LSS_{max} [MPa]	QDNSS [MPa]	$QDNSS_{max}$ [MPa]
73 ± 5	43 ± 4	50	68 ± 2	70

Quasi-DNS testing could therefore be a substitute for SLS testing. In addition to a better assessment of the mode II loading, this can lead to cost saving due to smaller specimen sizes and cheaper equipment.

To study the influence of roughness on UW, two surface conditions were tested on the PEI side of the plates. One was generated by thermocompression in contact with a sandblasted backplate (SDB), and the other one with a shotblasted one (STB). The roughness of each specimen was measured before welding. The range is quite large on these specimens: between 9 and 32 μm . The substrates were classified to have pairs of equivalent values. The reference specimens were standard ones (STD), meaning they had a relatively smooth PEI energy director. Their arithmetic roughness was measured between 0.2 and 0.4 μm . The optimized welding parameters for the standard specimens were kept for the rough ones. After welding, the joints were tested in SLS. The results shown in Fig. 4A demonstrate that the higher the roughness, the lower the apparent LSS. Moreover, a high deviation in the results is pointed out. After visual inspection of the fractured surfaces of most joints fractured below 20 MPa, it appears that these welds are incomplete, which means that some portions of the welding area are still intact, and the fracture is located within the energy director. To obtain the true LSS of assemblies, image processing in ImageJ software gives access to the true welded area. The latter is then reported to the true LSS value and plotted versus the roughness in Fig. 4B. A plateau at around 22 ± 4 MPa is identified, which corresponds to the minimum lap shear strength of the weld for these materials, regardless their roughness. Nevertheless, when comparing STB and SDB backplates specimens with STD ones, there is a real gap in roughness, respectively with a minimum value of around 10 μm for rough specimen, and a maximum value of 0.4 μm for smooth ones. Thus, a roughness threshold shall exist between both values, and the fluctuation from 0.4 μm to this threshold should be interesting to study. Unfortunately, no intermediate data are available for this study.

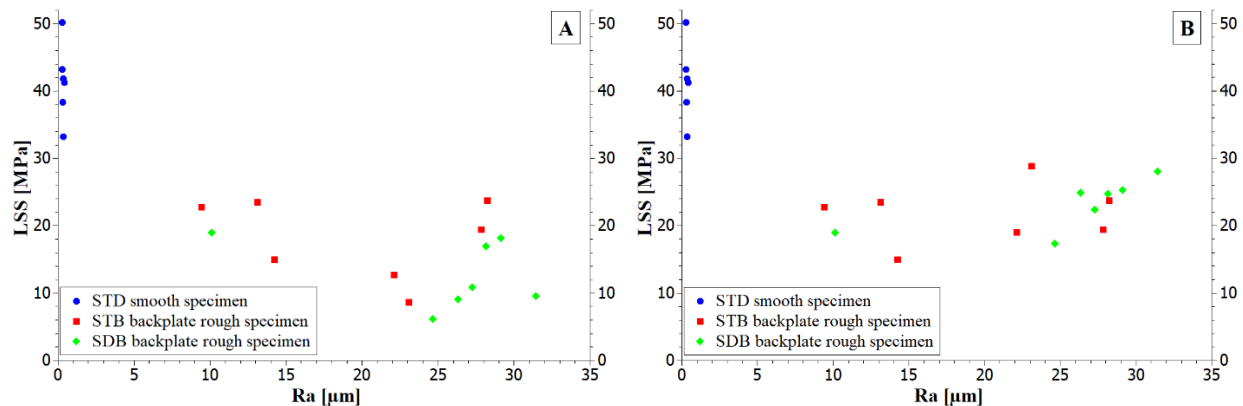


Fig. 4. (A) LSS of CF/PEEK assemblies as a function of PEI energy director roughness. (B) The same results obtained by using the true welded areas in the strength calculation.

To go deeper towards understanding such results, the welding curves are closely examined and compared with the obtained roughness and LSS values. Fig. 5 shows typical welding curves, which highlight the sonotrode displacement over time and the dissipated power during welding. The curves show the main characteristic stages of ultrasonic welding as described by Villegas [8] with slight variations due to different tooling and welding configuration, namely, stage 1) heating of the energy director, stage 2) after a first peak of dissipated power, energy director starts to melt, stage 3) the entire energy director is in a molten state and the sonotrode begins its main displacement, stage 4) includes a second power peak, the matrix at the contact of the energy director starts to melt locally, and stage 5) the matrix at the interphase is completely molten and the degradation begins due to overheating, while the dissipated power starts decreasing.

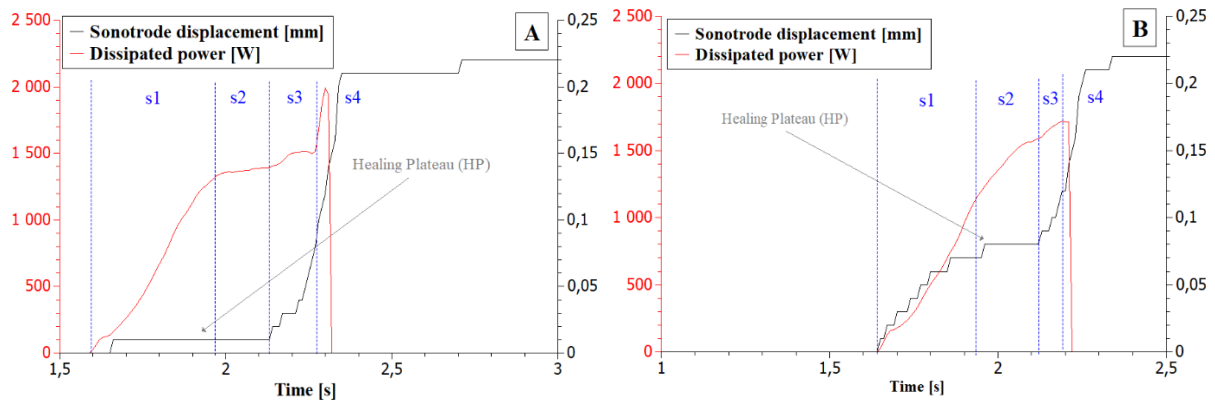


Fig. 5. Welding curves showing sonotrode displacement and dissipated power versus time. Typical curves for (A) standard specimens, (B) rough specimens.

The reference specimens led to the best results by reaching the middle or end of stage 4, which usually involves the joint fracture located within the composite plies. For the rough ones, the welding process more frequently stops during stage 3 or at the very beginning of step 4, and the break often takes place inside the energy director. However, significant differences appear between these graphs' displacement curves. The welding of rough specimens revealed a clearly visible plateau on the displacement curve during stage 1 and 2, which is obvious for all specimens. To date, this phenomenon has never been mentioned in the literature, probably because no study has focused on assembling rough surfaces until now, but smooth specimens. It is similar to fluctuations surrounding the initial point of displacement. However, the sonotrode displacement in stage 1 indicates that this plateau is representative of the beginning of the intimate contact between the welded surfaces. In the following, it will be called *Healing Plateau (HP)*. *Intimate contact time* (t_{ic}) is identified as the time required to reach this plateau. Fig. 5b shows a significant power requirement to heat the substrate interfaces and flatten the surface asperities. In this case, rather than getting a first power peak, the change in slope seems to match with the stage 2 transition, which occurs during the HP. In the examples shown, the HP of rough specimens lasts slightly less than half as long as for smooth specimens (here, $t_{HPsmooth} = 0.53$ s and $t_{HPrough} = 0.24$ s).

There is another important point to consider. In displacement mode in USW, the requested final height arrives too quickly, this is why stage 4 is scarcely reached. The sonotrode travelled distance to reach the plateau is a loss which prevents from achieving the requested displacement and thus, obtain an efficient joining. The roughness could help predicting the height of HP and t_{ic} , as shown in Fig. 6. There seems to be a trend for all roughnesses, but with significant variability for the lowest ones. Therefore, it should be possible to adjust the welding distance depending on the roughness, in order to reach the desired height in displacement mode. For LSS values below 10 MPa, identifying the HP is not obvious.

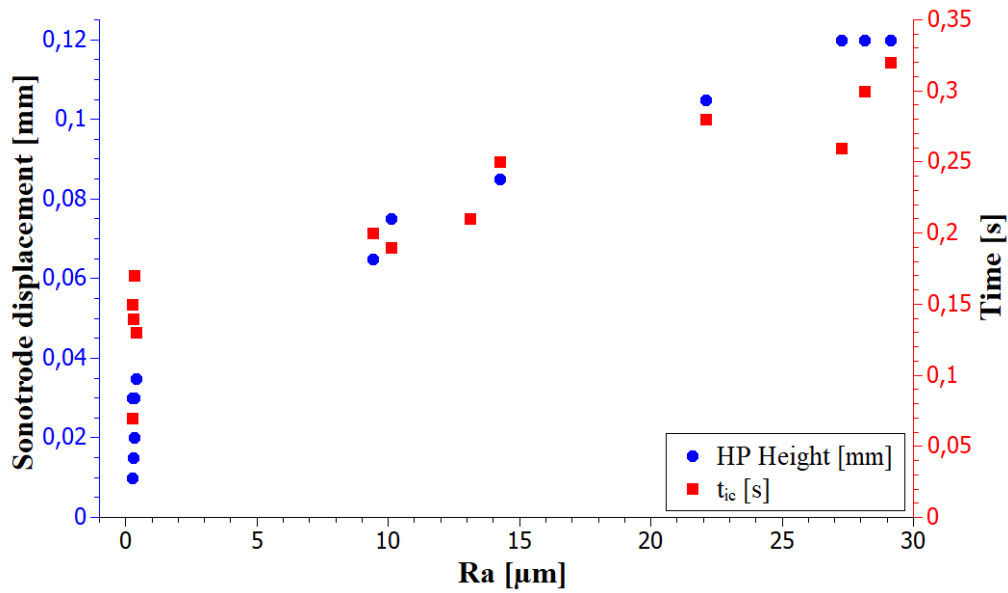


Fig. 6. Healing plateau height position (rounds) and experimental intimate contact time (squares), defined from the welding curves during sonotrode displacement for assemblies with $LSS > 10$ MPa.

The *healing plateau duration* (t_{HP}), which is finally a characteristic heating time of the interphase, could therefore be responsible for the strength of the assemblies. All plateau durations were measured on the welding curves, using a first-order derivative function to highlight the displacement variations. These results were scaled to the weld area and compared to each joint resistance in Fig. 7. A proportionality appears between t_{HP} and the LSS values. This trend seems to imply that t_{HP} should be maximized to obtain the best welding results. This finding, if confirmed by further studies, could be a simple and non-destructive way of assessing the quality of an ultrasonically welded joint.

To go further in the analysis, the *healing time* (t_h) and t_{HP} are highlighted. It is expected these two values are related. Assuming t_{rep} is considered unitary, and the shear stress of the bulk in SLS is fixed to our maximum value LSS_{max} , the shear stress and time ratios were calculated and plotted in Fig. 8 according to Eq. 4. The resulting trend looks like a line that does not pass through the origin, suggesting t_{HP} is different from t_h .

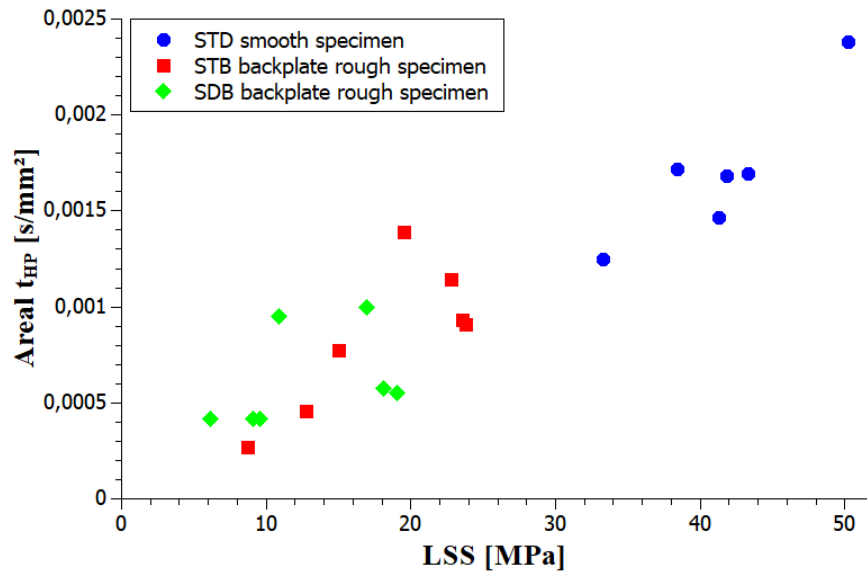


Fig. 7. Link between the healing plateau duration and the shear strength of welded assemblies.

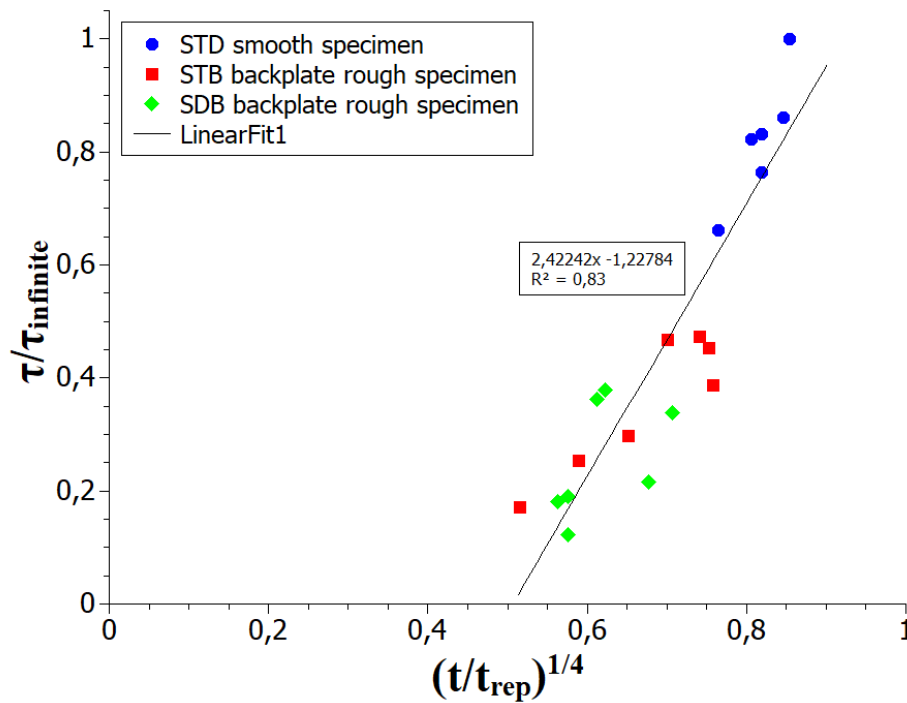


Fig. 8. Healing degree obtained by plotting shear stresses versus time ratios.

Summary

The influence of roughness when assembling composite plates by ultrasonic welding was studied. For that, composite specimens were manufactured with various roughness. For the first time, the intimate contact time was identified experimentally through the power and displacement welding curves. The displacement curves revealed a characteristic plateau duration, particularly evident on rough surfaces, which appears to be directly related to the joint shear strength. Exploiting this knowledge is a first step towards non-destructive examination of assemblies. It was established that this characteristic time is not the healing time of the interface during welding, but the link

between them seems obvious. A high roughness seems to have a negative effect on the strength of a joint welded in displacement mode by USW.

Finally, DNS test as a method of assessing Mode II strength has proven to be more reliable than SLS test, in addition to being less costly in terms of equipment and materials. Nevertheless, it can be established that an SLS test resulting in an LSS/SS_{bulk} ratio of 60% or more demonstrates the high quality of an assembly.

Acknowledgments

This work received financial support from ANR through France Relance plan of the French government in collaboration with the company Lauak Group (France).

References

- [1] S.S. Voyutskii, V.L. Vakula, The role of diffusion phenomena in polymer-to-polymer adhesion, *J. Appl. Polym. Sci.* 7 (1963) 475-491. <https://doi.org/10.1002/app.1963.070070207>
- [2] W.I. Lee, G.S. Springer, A Model of the Manufacturing Process of Thermoplastic Matrix Composites, *J. Compos. Mater.* 21 (1987) 21. <https://doi.org/10.1177/002199838702101103>
- [3] F. Yang, R. Pitchumani, A fractal Cantor set based description of interlaminar contact evolution during thermoplastic composites processing, *J. Mater. Sci.* 36 (2001) 4661-4671. <https://doi.org/10.1023/A:1017950215945>
- [4] P.G. de Gennes, Reptation of a Polymer Chain in the Presence of Fixed Obstacles, *J. Chem. Phys.* 55 (1971) 572. <https://doi.org/10.1063/1.1675789>
- [5] D. Adolf, M. Tirrell, Molecular weight dependence of healing and brittle fracture in amorphous polymers above the entanglement molecular weight, *J. Polym. Sci.: Polym. Phys. Ed.* 23 (1985) 413-427. <https://doi.org/10.1002/pol.1985.180230214>
- [6] S. Prager, M. Tirrell, The healing process at polymer-polymer interfaces, *J. Chem. Phys.* 75 (1981) 5194. <https://doi.org/10.1063/1.441871>
- [7] Y.H. Kim, R. P. Wool, A theory of healing at a polymer-polymer interfaces, *Macromolecules* 16 (1983) 1115-1120. <https://doi.org/10.1021/ma00241a013>
- [8] I.F. Villegas, Strength development versus process data in ultrasonic welding of thermoplastic composites with flat energy directors and its application to the definition of optimum processing parameters, *Compos. Part A: Appl. Sci. Manuf.* 65 (2014) 27-37. <https://doi.org/10.1016/j.compositesa.2014.05.019>